

Conference Title

ASI Conference Series, 2011, Vol. 00, pp 1–5

Editors:



## Spectroscopic investigation of SDSS J100921.40+375233.9 selected from SDSS and GALEX photometry

Timur Şahin<sup>1,2,3\*</sup>, David L. Lambert<sup>3</sup> and Carlos Allende Prieto<sup>4,3</sup>

<sup>1</sup>Department of Space Science and Technologies, Akdeniz University, Antalya, 07058, TURKEY

<sup>2</sup>TUBITAK National Observatory, Akdeniz University Campus, Antalya, 07058, TURKEY

<sup>3</sup>Department of Astronomy and The W. J. McDonald Observatory, University of Texas, Austin, TX 78712, USA

<sup>4</sup>Instituto de Astrofísica de Canarias, 38205, La Laguna, Tenerife, SPAIN

Received 12th November 2018

### Abstract.

In this study, we aim to reveal the nature of the Sloan Digital Sky Survey (SDSS) star: SDSS J100921.40+375233.9, suspected to have an extremely low metallicity. We observed this star at high spectral resolution and performed an abundance analysis. We derived the spectroscopic parameters  $T_{eff} = 5820 \pm 125$  K,  $\log g = 3.9 \pm 0.2$ , and  $\xi_t = 1.1 \pm 0.5$  km s<sup>-1</sup>. The star is consistent with belonging to the thick disk.

*Keywords* : Stars: abundances – Stars: atmospheres

## 1. Introduction

Making use of the tables of cross-matched sources between Galaxy Evolution Explorer (GALEX) and SDSS available at the Multimission Archive at the Space Telescope (MAST), we have identified stars that exhibit colors of extremely metal-poor stars.

Figure 1. is a combination of GALEX and SDSS photometry, i.e., a stellar density map in the plane of the  $NUV - g$  and  $z - g$  colors for a sample of some 200,000 stars and reveals two accumulations of sources: one centered at  $z - g = -0.47$  and  $NUV - g = 3.7$  and associated with moderately metal-poor F and G main sequence

\*email: timursahin@akdeniz.edu.tr

and subgiant stars. The second cluster at a similar  $z - g$  but at  $NUV - g \simeq 2.7$  is populated by white dwarfs. We have used the  $g$ ,  $z$  and  $NUV$  colors of BD +17 4708 to set the zero point of the  $z - g$  and  $NUV - g$  scales for model fluxes from Kurucz's model atmospheres (Kurucz 1993). For the photometry of BD +17 4708, the fluxes are taken from Bohlin & Gilliland (2004). After this calibration, the calculated colours for a similar subgiant in the range of effective temperature between 5900–6400 K with metallicities typical of the thin disk ( $[Fe/H]=0$ ), the thick disk ( $[Fe/H]= -0.7$ ), halo ( $[Fe/H]=-1.5$ ), and ultra-low metallicity ( $[Fe/H]= -4.5$ ) population, are shown in Fig. 1. with solid lines. The same models for a dwarf star ( $logg = 5$ ) correspond to the dashed lines in the figure.

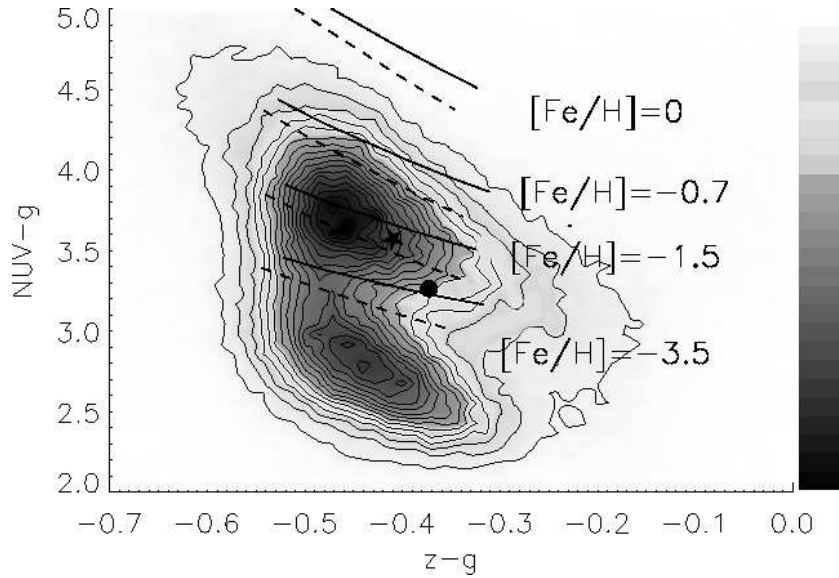


**Figure 1.** A stellar density map for a sample of 200,000 stars which are photometrically similar to the flux standard BD+17 4708 (indicated with a star symbol). Filled circle represents J100921.

## 2. Observations

High-resolution spectra for SDSS J100921 High-resolution spectra for SDSS J100921 (SDSS J100921.40+375233.9 = HIP 49750 = NLTT 23519) were obtained on 2009 March 15 (two frames) at the McDonald observatory with the 2.7 meter Harlan J. Smith reflector with the CCD-equipped Tull cross-dispersed échelle spectrograph (Tull et al. 1995). The spectra have a FWHM resolving power of  $\lambda/\delta\lambda \simeq 60,000$  with full spectral coverage from 3600 to 5300 Å, and substantial but incomplete coverage from 5300 to 10 200 Å.

**Table 1.** Abundances of the observed species for SDSS J100921, J171422, and J015717 are presented for the model atmospheres of  $T_{\text{eff}} = 5820$  K,  $\log g = 3.9$ ,  $\xi = 1.1$  and  $T_{\text{eff}} = 6320$  K,  $\log g = 4.1$ ,  $\xi = 1.5$ , and  $T_{\text{eff}} = 6250$  K,  $\log g = 3.7$ ,  $\xi = 4.0$ , respectively. The solar abundances from Asplund et al. (2009) are used to convert the abundance of element X to  $[X/\text{Fe}]$ .

Species	J100921			$\log \epsilon_{\odot}$	Species	J100921			$\log \epsilon_{\odot}$
	$\log \epsilon(X)$	[X/H]	[X/Fe]			$\log \epsilon(X)$	[X/H]	[X/Fe]	
<i>Li</i> I	1.76	0.71	+2.01	1.05	<i>Cr</i> I	4.32	-1.32	-0.02	5.64
<i>C</i> I	7.58	-0.85	+0.45	8.43	<i>Cr</i> II	4.48	-1.16	+0.14	5.64
<i>O</i> I	8.28	-0.41	+0.89	8.69	<i>Mn</i> I	3.91	-1.52	-0.22	5.43
<i>Na</i> I	5.20	-1.04	+0.26	6.24	<i>Fe</i> I	6.20	-1.30	+0.00	7.50
<i>Mg</i> I	6.56	-1.04	+0.26	7.60	<i>Fe</i> II	6.20	-1.30	+0.00	7.50
<i>Al</i> I	5.07	-1.38	-0.08	6.45	<i>Co</i> I	3.98	-1.01	+0.29	4.99
<i>Si</i> I	6.45	-1.06	+0.24	7.51	<i>Ni</i> I	4.99	-1.23	+0.07	6.22
<i>Ca</i> I	5.18	-1.16	+0.14	6.34	<i>Zn</i> I	3.36	-1.20	+0.10	4.56
<i>Sc</i> II	2.06	-1.09	+0.21	3.15	<i>Sr</i> II	1.58	-1.29	+0.01	2.87
<i>Ti</i> I	3.87	-1.08	+0.22	4.95	<i>Y</i> II	0.87	-1.34	-0.04	2.21
<i>Ti</i> II	4.08	-0.87	+0.43	4.95	<i>Zr</i> II	1.44	-1.14	+0.16	2.58
<i>V</i> I	2.59	-1.34	-0.04	3.93	<i>Ba</i> II	0.98	-1.20	+0.10	2.18
<i>V</i> II	2.82	-1.11	+0.19	3.93					

Observations were reduced using the echelle reduction package in IRAF. We refer the reader to Şahin et al. (2011) for details of data reduction.

We determined the heliocentric radial velocity of our target as  $V_{\odot} = -59.3 \pm 0.5$  km s<sup>-1</sup>. A section of the final spectrum is shown in Figure 2.

### 3. Spectral Analysis

The abundance analysis was undertaken with models obtained by interpolating in the ATLAS9 model atmosphere (ODFNEW models) grid (Castelli & Kurucz 2003) and the line analysis programme MOOG (Snedden 2002). The models are line-blanketed plane-parallel atmospheres in Local Thermodynamical Equilibrium (LTE) and hydrostatic equilibrium with flux (radiative plus convective) conservation and computed with a constant microturbulent velocity ( $\xi = 2$  km s<sup>-1</sup>).

The original sources for the transition probabilities of the Fe I lines are listed by Lambert et al. (1996). The  $gf$  values for Fe II lines are taken from Meléndez et al. (2006).

The model parameters were determined using only spectroscopic criteria. Iron is used to obtain an estimate of  $\log g$ . Finally, the metallicity  $[\text{Fe}/\text{H}]$  is refined by

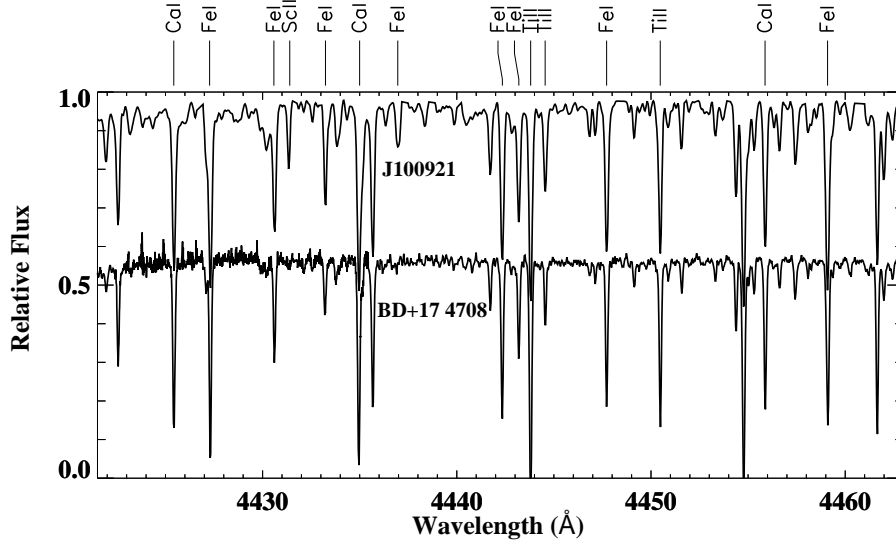


**Figure 2.** The velocity corrected spectra of SDSS J100921 and BD +17 4708. Selected lines are identified.

requiring that the derived abundance be equal to that adopted for the construction of the model atmosphere for the final set of  $T_{\text{eff}}$ ,  $\log g$ , and  $\xi$ . For details of the spectral analysis, we refer the reader to Şahin et al. (2012, in preparation).

The model atmosphere parameters found for the star are  $T_{\text{eff}} = 5820 \pm 125$  K,  $\log g = 3.9 \pm 0.2$ , and  $\xi_t = 1.1 \pm 0.5$  km s $^{-1}$

#### 4. Concluding Remarks

We performed the first detailed abundance analysis on SDSS J100921 for 21 elements. A summary of the abundances for the star is given in Table 1, where the quantities  $\log \epsilon(X)$ ,  $[X/H]$ , and  $[X/Fe]$  are reported in columns two, three, and four.

SDSS J100921.40+375233.9 appears to lie close to ultra-low metallicity ( $[Fe/H] = -3.5$ ) population track (Fig 1.), with the fact that the SDSS photometry for the star is saturated. Despite of the high risk, we have followed spectroscopically the target to explore the nature of the star in detail.

On the basis of preliminary results, we report that SDSS J100921.40+375233.9 do not present ultra-low metallicity and is roughly consistent with thick-disk membership.

### **Acknowledgements**

I thank to Royal Astronomical Society (RAS) for providing the funds to attend the meeting.

### **References**

- Bohlin R. C., Gilliland R. L., 2004, *AJ*, 128, 3053  
Snedden, C., 2002, MOOG An LTE Stellar Line Analysis Program  
Şahin T., Lambert D. L., Klochkova V. G., Tavganskaya S., 2011, *MNRAS*, 410, 612  
Tull R. G., MacQueen P. J., Sneden C., Lambert D. L., 1995, *PASP*, 107, 251